

# The Impact of Cathode Material and Shape on Current Density in an Aluminum Electrolysis Cell

YANG SONG,<sup>1</sup> JIANPING PENG,<sup>1,2</sup> YUEZHONG DI,<sup>1</sup> YAOWU WANG,<sup>1</sup>  
BAOKUAN LI,<sup>1</sup> and NAIXIANG FENG<sup>1</sup>

1.—School of Metallurgy, Northeastern University, Shenyang 110819, China. 2.—e-mail: pengjp@smm.neu.edu.cn

A finite element model was developed to determine the impact of cathode material and shape on current density in an aluminum electrolysis cell. For the cathode material, results show that increased electrical resistivity leads to a higher cathode voltage drop; however, the horizontal current is reduced in the metal. The horizontal current magnitude for six different cathode materials in decreasing order is graphitized, semi-graphitized, full graphitic, 50% anthracite (50% artificial graphite), 70% anthracite (30% artificial graphite), 100% anthracite. The modified cathode shapes with an inclined cathode surface, higher collector bar and cylindrical protrusions are intended to improve horizontal current and flow resistance. Compared to a traditional cathode, modified collector bar sizes of 70 mm × 230 mm and 80 mm × 270 mm can reduce horizontal current density component  $J_x$  by 10% and 19%, respectively, due to better conductivity of the steel. The horizontal current in the metal decreases with increase of cathode inclination. The peak value of  $J_x$  can be approximately reduced by 20% for a 2° change in inclination. Cylindrical protrusions lead to local horizontal current increase on their tops, but the average current is less affected and the molten metal is effectively slowed down.

## INTRODUCTION

Primary aluminum is produced through the electrolysis process. Direct electric current flows from anodes to the liquid aluminum layer through cryolite, in which alumina is dissolved.<sup>1</sup> The current is almost vertical in the bath layer due to its low conductivity, but a horizontal current establishes when the current enters the highly conductive metal layer. After the metal pad, the current flows into the cathode and is conveyed by collector bars to external bus bars. These bus bars carry the current to feed the anode rods of the next cell.

A great amount of energy is consumed during electrolysis, especially lost into Joule heat in the cryolite layer. So keeping the anode–cathode distance (ACD) as small as possible can reduce energy consumption. Unfortunately, the bath–metal interface is not flat due to the metal flow driven by magnetohydrodynamic (MHD) forces. The metal waves appear in a similar way to the waves on the surface of lakes and seas. So one of the principal

barriers is that ACD below a certain threshold value would lead to unstable waves, which makes the reduction of ACD hard to achieve from the current ACD 4 cm even in modern carefully designed cells.<sup>2</sup>

The MHD forces due to the vertical magnetic component ( $B_z$ ) interacting with the horizontal current in the metal ( $J_x$ ) are the sources of instability.<sup>3</sup> There have been many investigations regarding reducing MHD forces.

Studies<sup>4–9</sup> on magnetic compensation and velocity field control of the molten liquids have shown significant progress. These studies have elucidated that side risers can compensate for vertical magnetic fields ( $B_z$ ) and increase flow resistance so as to reduce voltage oscillation.

Some investigations have focused on design modifications to the cathode in order to make the current density more uniform.<sup>10–14</sup> The investigations have indicated satisfactory results in reducing peak values of the current density. In addition, authors have reported on the impact of inclined

sidewall design<sup>15</sup> on MHD forces, anode shape<sup>16</sup> on current density, and anode connector<sup>17</sup> on voltage drop, which are of importance when creating a new or modifying an existing design of a reduction cell. But none of these studies refer to cathode material.

According to cited studies, incorporated multiple side risers for magnetic compensations, inclined/slotted large anodes with optimized stub design, and a point feeder system that can control shot size, the performance of cells has improved to 95–96% current efficiency and in some cases has achieved 13,500 DC kWh/t of energy consumption.<sup>15</sup>

Inspired by the piles in inshore waters to reduce the intensity of wave action, a plane cathode with cylindrical protrusions was proposed and tested in 2010. After 2 years, industrial tests demonstrated that this novel cathode could reduce energy consumption to 12,400 kWh/t(AL), 600–1000 kWh/t (AL) less than a traditional cell.<sup>18</sup> The purpose of the protrusions is to directly reduce metal flow. However, the drawback of the design is that the horizontal current in the metal has not been considered.

This work concentrates on examining the impact of cathode material and shape, which are intended to improve horizontal current density and flow resistance simultaneously.

## MODELS

In this analysis, an entire three-dimensional electrolysis cell was modeled in ANSYS. The Three-dimensional (3D) electrolysis cell model is illustrated in Fig. 1. The upstream and downstream vertical bus bars are modeled but without adjacent cells. The cell has 40 anodes and 26 cathodes. All these components in Fig. 1 are surrounded by a large cubic air (not shown in this geometry) in the magnetic field calculations. In this study, 11,97,560 elements and 16,48,151 nodes were used in the cell with the flat cathode.

The following parameters are considered for the cell in Table I.

For electromagnetic analysis in ANSYS, electric potential  $V$  is solved from the Laplace equation.

$$\nabla \cdot (\sigma \nabla V) = 0 \quad (1)$$

where  $\sigma$  is the electrical conductivity and  $V$  is the electric potential.

The current density  $\mathbf{J}$  is calculated from Eq. 2.

$$\mathbf{J} = -\sigma \nabla V \quad (2)$$

The magnetic field is calculated using Maxwell equations.

$$\nabla \times \mathbf{H} = \mathbf{J} \quad (3)$$

$$\mathbf{B} = \mu \mathbf{H} \quad (4)$$

where  $\mathbf{H}$  is magnetic field strength,  $\mathbf{B}$  is the magnetic induction,  $\mathbf{J}$  is the current density, and  $\mu$  is the permeability.

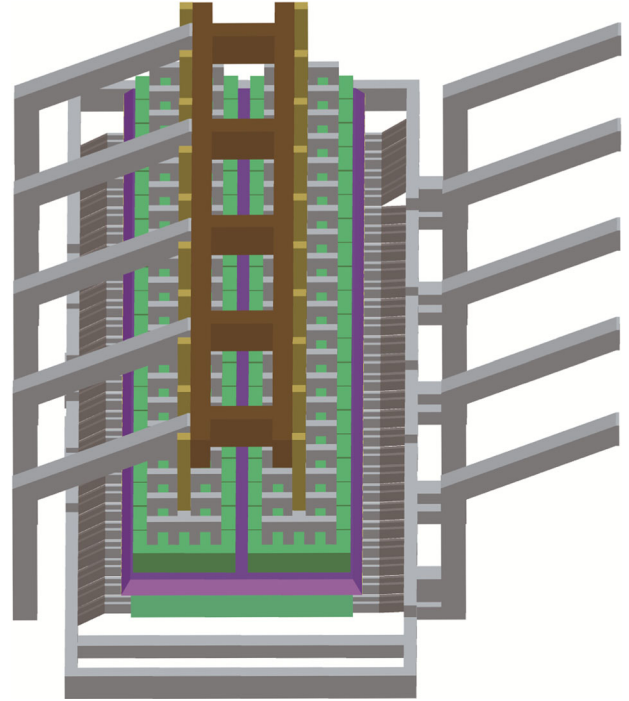


Fig. 1. Geometry of the 3D electrolysis cell model.

Table I. Cell parameters

Cell parameters	
Anode dimension Length × width × height	1550 mm × 660 mm × 600 mm
Cathode dimension Length × width × height	3420 mm × 515 mm × 450 mm
Collector bar	65 mm × 180 mm
Metal height	280 mm
Bath height	215 mm
Anode cathode distance (ACD)	50 mm
Line current	300 kA
Steel resistivity	7.78 μΩ m

The Lorentz force resulting from the interaction of the electromagnetic fields is given by the following:

$$\mathbf{F}_{EM} = \mathbf{J} \times \mathbf{B} \quad (5)$$

The following assumptions are made to simplify the calculations:

- (1) Each vertical upstream bus bar shares the same current.
- (2) The electrical resistances of the cathodes and steel collector bars are taken as constant, which are model limitation.
- (3) Electrical contact resistance and resistive heating are not considered.
- (4) Steady state conditions are adopted.

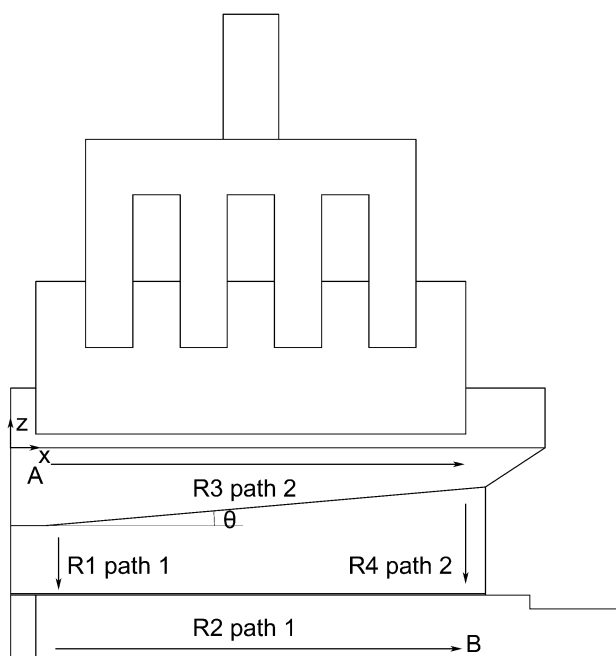


Fig. 2. Sectional plane of inclined cathode.

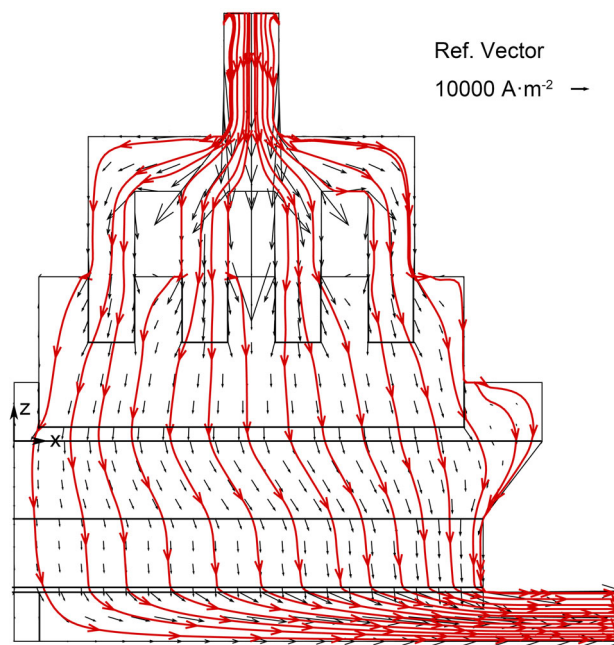


Fig. 3. Current distribution of the  $x$ - $z$  plane in the traditional cell.

**Boundary conditions**

- (1) For the current field: 0 V reference potential on each outlet of the downstream vertical bars.
- (2) For the magnetic field: Flux in parallel to air external on areas.
- (3) For the flow field: The fluid boundaries with the ledge, anodes and the top of the cathode are all set to no slip walls.

Figure 2 represents the sectional plan of the inclined cathode, proposed by Feng in 2011.<sup>19</sup>  $R1$  and  $R2$  are the resistances of cathode and collector bar in path 1, respectively,  $R3$  and  $R4$  are the resistances of aluminum and cathode in path 2, respectively,  $I_1$  and  $I_2$  are the currents in path 1 and path 2, respectively, and  $\theta$  is the cathode inclination.

The voltage drop between A and B is the same when the current flows through path 1 or path 2 (Eqs. 6 and 7).

$$I_1(R1 + R2) = I_2(R3 + R4) \tag{6}$$

$$\frac{I_2}{I_1} = \frac{R1 + R2}{R3 + R4} \tag{7}$$

Increasing the resistance of the cathode in path 2  $R4$  and reducing the resistance of the collector bar  $R2$  will reduce the horizontal current  $I_2$  in aluminum if other parameters are constant. So cathode inclination and higher collector bar have been attempted to make the horizontal current more uniform.

**RESULTS AND DISCUSSION**

**Current Distribution**

Figure 3 shows the current distribution of the  $x$ - $z$  plane in the traditional cell.

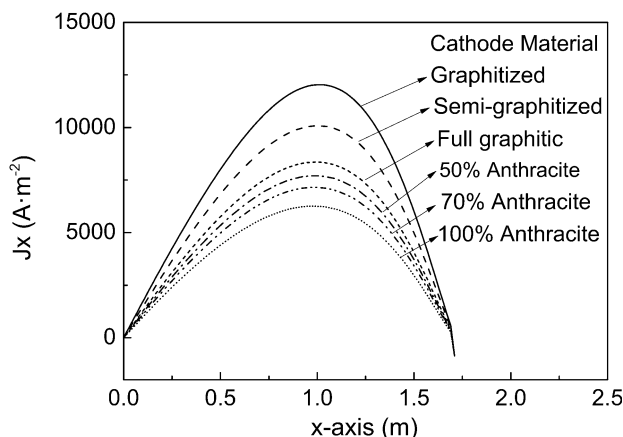


Fig. 4. Horizontal current density component  $J_x$  in the plane situated 4 cm under the bath-metal interface for different cathode materials.

The current tends to flow through the path of least resistance. Attributed to high resistivity of the cryolite, the current remains mostly vertical in the bath and little current appears near the sidewall. When the current enters the highly conductive molten metal, it runs askew and flows toward the sidewall, creating a high horizontal current component in the metal.

**Cathode Material Effect**

The cathode voltage drop and current density were calculated for six different cathode materials. Figure 4 and Table II show the impact of the cathode material.

**Table II. Cathode voltage drop (CVD) and horizontal current density components  $J_x$  in the plane situated 4 cm under the bath-metal interface for different cathode materials**

Cathode material	Resistivity ( $\mu\Omega \text{ m}$ )	CVD (mV)	$J_x \text{ max}$ ( $\text{J m}^{-2}$ )
Graphitized	12	230	12,039
Semi-graphitized	20	258	10,082
Full graphitic	30	288	8356
50% anthracite, 50% artificial graphite	35	302	7706
70% anthracite, 30% artificial graphite	40	316	7153
100% anthracite	50	341	6217

The horizontal current increases to a peak at about 2/3 of half-cathode length from the center, and then decreases to a negative value due to the presence of the inclined sidewall. Among the six cathodes, graphitized cathodes establish the least cathode voltage drop and the largest horizontal current in the metal. Increased electrical resistivity leads to a higher cathode voltage drop; however, the horizontal current is reduced in the metal. For the 100% anthracite cathode, the peak value of horizontal current density component  $J_x$  in the metal is almost half that of the graphitized cathode. Cathodes with anthracite as a raw material also possess a better erosion wear resistance property than other materials.<sup>20</sup> In comparison, graphitized cathodes have the best properties except for the high horizontal current and the worst erosion wear resistance property in these materials.

Throughout the rest of the calculations, 100% anthracite is adopted as the cathode material.

### Cathode Shape Effect

The steel collector bar size of a traditional plane cathode is  $65 \times 180 \text{ mm}$ . The modified sizes to reduce electrical resistance for comparison are  $70 \text{ mm} \times 230 \text{ mm}$  and  $80 \text{ mm} \times 270 \text{ mm}$ . The height of the outlets remain at 180 mm to reduce heat loss.

Figure 5 shows the impact of steel collector bar size on the horizontal current. It is predicted that, compared to a traditional cathode, modified collector bar sizes of  $70 \text{ mm} \times 230 \text{ mm}$  and  $80 \text{ mm} \times 270 \text{ mm}$  can reduce  $J_x$  by 10% and 19%, respectively, due to better conductivity of the steel.

Recently, authors<sup>3</sup> have reported that there is a 50% decrease in the peak value of current density while using copper collector bars because copper has very high electrical conductivity, which could be a better option than steel if the cell thermal balance is well maintained.

The angle of cathode inclination was varied from  $0^\circ$  to  $6^\circ$  (Fig. 6), providing four different designs. Increased electrical resistance in the cathode sides alters the current path and the current is redistributed. It is obvious that the horizontal current decreases with the increase of cathode inclination. The peak value of  $J_x$  can be approximately reduced by 20% for  $2^\circ$  changes in inclination.

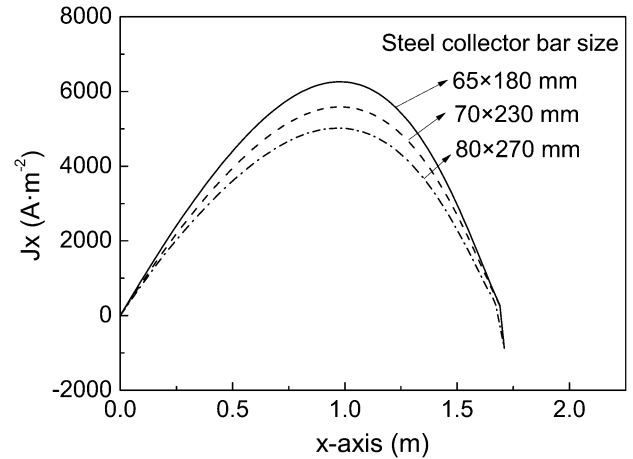


Fig. 5. Horizontal current density component  $J_x$  in the plane situated 4 cm under the bath-metal interface for different collector bar sizes.

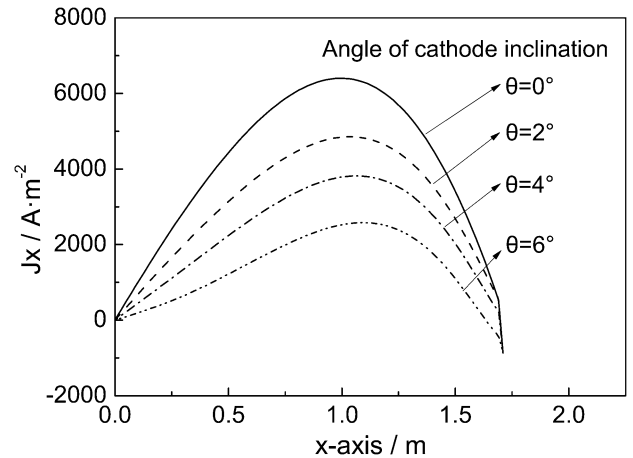


Fig. 6. Horizontal current density component  $J_x$  in the plane situated 4 cm under the bath-metal interface for different cathode surface inclinations.

Reny<sup>21</sup> reported that a higher local current seems to accelerate cathode wear. Wear is found to be severe in high-velocity regions where current densities are relatively higher.<sup>22,23</sup> The location of the higher current density in the metal corresponds to the location where the cathode is wearing faster



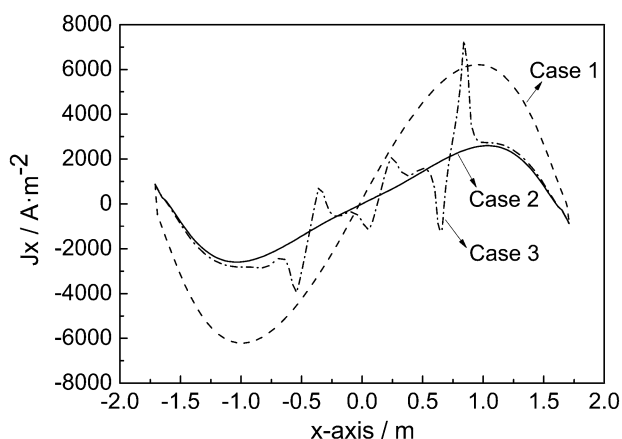


Fig. 7. Horizontal current density component  $J_x$  at the mid height of the metal (line CD in Fig. 8) for different cathode shapes.

(close to the side of the cathode<sup>21</sup>). Therefore, the higher cathode side is expected to be beneficial to reduce wear to prolong cathode life.

### Combined Modified Cathode Shape Effect

As mentioned previously, the plane cathode with cylindrical protrusions can reduce metal flow, but the current has yet to be considered. Since metal thermal stability would be better with more metal volume and having higher metal level above the protrusions would improve longevity, a 5° inclination was adopted for further calculations.

So, in this work, combining the cathode modifications with the intention of reducing the horizontal current with the previous design, three cases were calculated to obtain the combined influence.

Case 1: traditional plane cathode

Case 2: modified cathode with 5° inclination and higher collector bar (70 mm × 230 mm)

Case 3: modified cathode with 5° inclination, higher collector bar (70 mm × 230 mm) and cylindrical protrusions

Figure 7 shows the horizontal current density component  $J_x$ . The current density in case 3 does not represent an average of the block width but only indicates the value at the line CD in Fig. 8. Comparing case 2 and case 1, the combination of cathode inclination and higher collector bar causes a 61% decrease in maximum  $J_x$ , in which the contribution of cathode inclination dominates. According to case 2 and case 3, the presence of carbon cylinders does not affect the average  $J_x$  very much, but on the tops of cylinders,  $J_x$  is extremely high. The carbon cathode is 100 times more resistive than aluminum, so when encountering the tops of the carbon cylinders, most current is divided into different directions and flows through the least resistive path in the metal rather than into the carbon cylinders, causing a large horizontal current.

Figure 9 gives the current distribution in the cathode assembly. The modified cathode makes the skew of the streamline less severe in case 2.

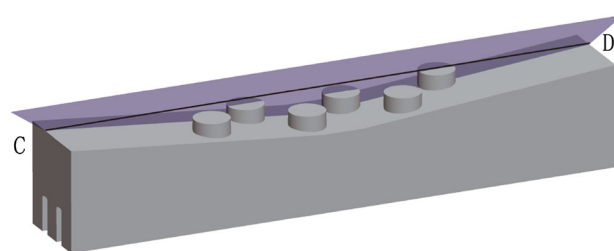


Fig. 8. Modified cathode with 5° inclination, higher collector bar size of 70 mm × 230 mm and cylindrical protrusions, line CD is at the mid height of the metal, above the tops of the cylindrical protrusions and parallel to longitudinal direction of cathode.

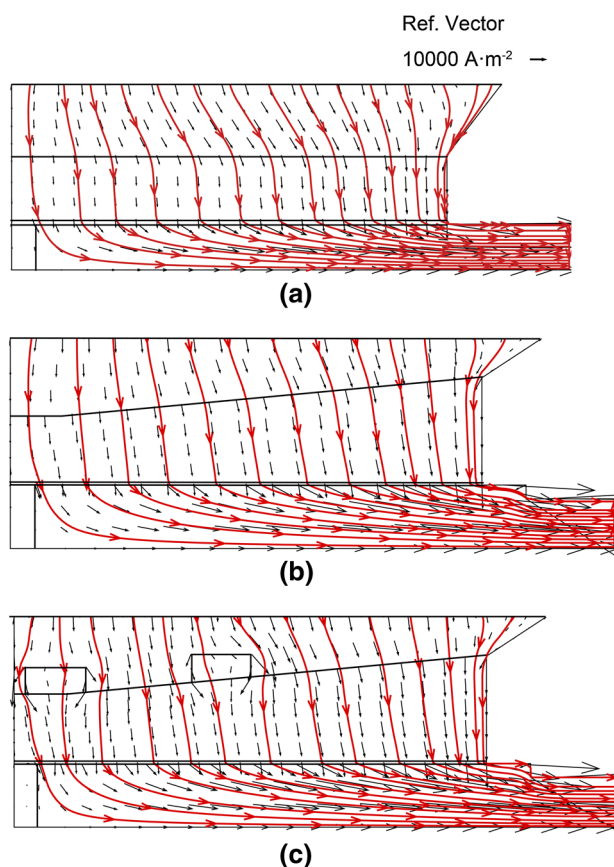


Fig. 9. Current vector and streamline in the cathode assembly. (a) Traditional cell with plane cathode (collector bar size 65 mm × 180 mm). (b) Modified cathode with 5° inclination and higher collector bar (size 70 mm × 230 mm). (c) Modified cathode with 5° inclination and higher collector bar (size 70 mm × 230 mm) and cylindrical protrusions.

Currents flow around the highly resistive carbon cylinders, while little current follows the path into the carbon cylinders.

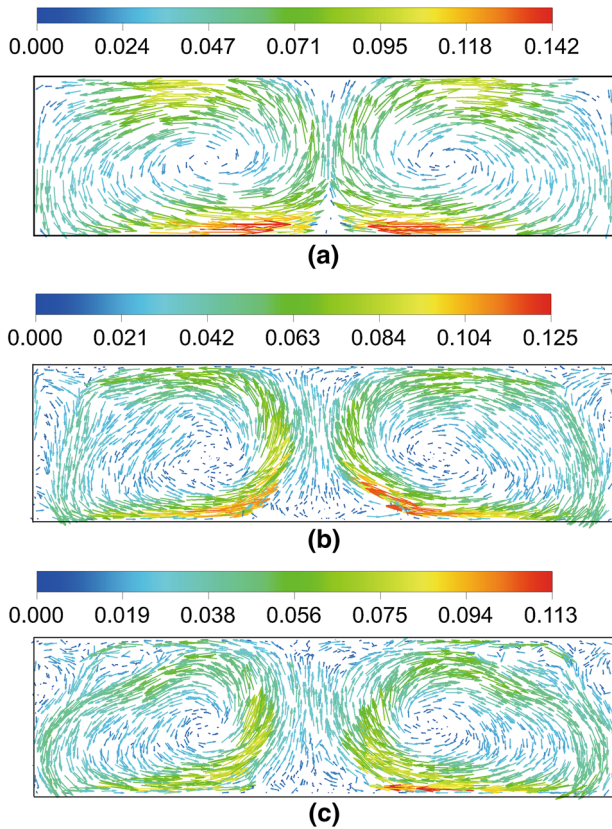


Fig. 10. Velocity profile in the cell in the plane situated 4 cm under the bath–metal interface (units:  $\text{m s}^{-1}$ ). (a) Traditional cell with plane cathode (collector bar size 65 mm  $\times$  180 mm). (b) Modified cathode with 5° inclination and higher collector bar (size 70 mm  $\times$  230 mm). (c) Modified cathode with 5° inclination and higher collector bar (size 70 mm  $\times$  230 mm) and cylindrical protrusions.

Figure 10 shows the impact of modified cathode shape on the metal flow, calculated in CFX driven by electromagnetic forces from ANSYS. The velocity reflects the combined effect of the modifications. Apparently, the inclined cathode surface and protrusions create a less intensive motion in the metal. The protrusions can redistribute the momentum and slow down the molten metal, transcending the drawback of making the current non-uniform on the tops. The interface deformation is primarily defined by the metal flow, which implies less deformation due to reduced metal flow.

Figure 11 gives the bath–metal interface deformation. Evidently, compared to the traditional cell, the inclined cathode surface and cylindrical protrusions are predicted to make the interface less deformed. In the real cell operation, the application of the novel cathode may reduce ACD. Nevertheless, several disadvantages regarding the modified shapes follow. The increased metal level due to the inclined cathode surface may affect the side ledge shape, which has not been considered in this paper. If ACD was reduced, the heat supply by the electrolyte would also be inadequate. The thermal balance and side ledge shape are probably affected

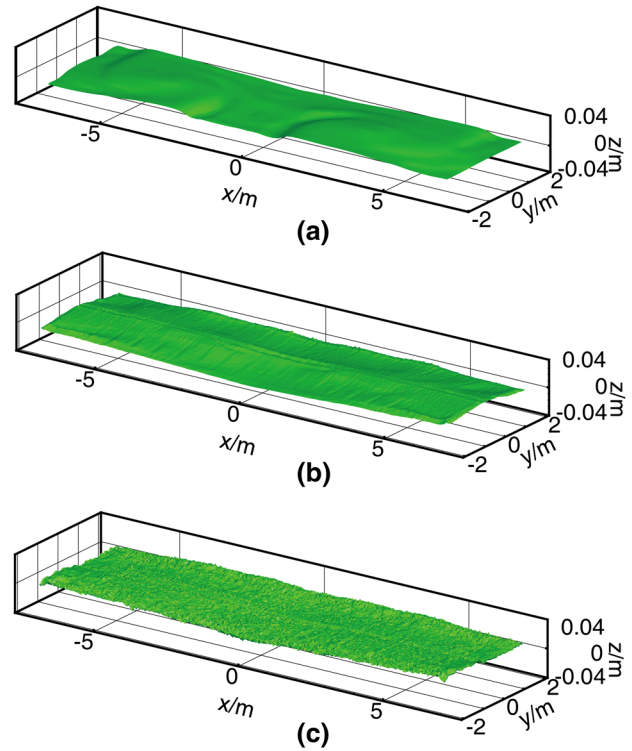


Fig. 11. Bath–metal interface deformation. (a) Traditional cell with plane cathode (collector bar size 65 mm  $\times$  180 mm). (b) Modified cathode with 5° inclination and higher collector bar (size 70 mm  $\times$  230 mm). (c) Modified cathode with 5° inclination and higher collector bar (size 70 mm  $\times$  230 mm) and cylindrical protrusions.

by the reduced electrolyte. So the full potential of the novel cathode can be reached by integrating strengthening insulation for the cell to maintain the thermal balance.

## CONCLUSION

A finite element model was developed to determine the impact of cathode material and shape on current density in an aluminum electrolysis cell.

- (1) For the cathode material, the results show that increased electrical resistivity leads to a higher cathode voltage drop; however, the horizontal current is reduced in the metal. The horizontal current magnitude for six different cathode materials in decreasing order is graphitized, semi-graphitized, full graphitic, 50% anthracite (50% artificial graphite), 70% anthracite (30% artificial graphite), 100% anthracite
- (2) The modified cathode shapes with inclined cathode surface, higher collector bar and cylindrical protrusions are intended to improve horizontal current and flow resistance. Compared to a traditional cathode, modified collector bar sizes of 70 mm  $\times$  230 mm and 80 mm  $\times$  270 mm can reduce  $J_x$  by 10% and 19%, respec-

- tively, due to better conductivity of the steel.
- (3) Horizontal current in the metal decreases with the increase of cathode inclination. The peak value of  $J_x$  can be approximately reduced by 20% for a  $2^\circ$  change in inclination.
  - (4) Cylindrical protrusions lead to local horizontal current increase on their tops, but the average current is less affected and the molten metal is effectively slowed down.

The modifications imply a very promising potential to reduce energy consumption, and cells equipped with modified cathodes in case 2 and 3 are now being tested, which will confirm the simulated results in the near future.

#### ACKNOWLEDGEMENTS

The authors are grateful for the financial support by the National Nature Science Foundation of China (Grant Nos. 51204044 and 51434005) and the National Key Technology R&D Program of China (No. 2015BAB04B03).

#### REFERENCES

1. N. Kandev and H. Fortin, *Light Metals*, ed. G. Bearne (Warrendale: TMS, 2009), pp. 1061–1066.
2. O. Zikanov, A. Thess, P.A. Davidson, and D.P. Ziegler, *Metall. Trans. B* 31, 1541 (2000).
3. S. Das, Y. Morsi, and G. Brooks, *JOM* 66, 235 (2014).
4. S. Das, G. Brooks, and Y. Morsi, *Metall. Trans. B* 42, 243 (2011).
5. M. Li, *J. Cent. South Univ. (Sci. Technol.)* 40, 562 (2009).
6. H. Sun, O. Zikanov, and D.P. Ziegler, *Fluid Dyn. Res.* 35, 255 (2004).
7. V. Bojarevics and K. Pericleous, *Light Metals*, ed. G. Bearne (Warrendale: TMS, 2009), pp. 569–574.
8. B. Li, *Light Metals*, ed. S.J. Lindsay (Warrendale: TMS, 2011), pp. 1029–1033.
9. B. Li, *Light Metals*, ed. C.E. Suarez (Warrendale: TMS, 2012), pp. 865–868.
10. S. Das and G. Littlefair, *Light Metals*, ed. S.J. Lindsay (Warrendale: TMS, 2011), pp. 847–851.
11. R. Kaenel and J. Antille, *Light Metals*, ed. S.J. Lindsay (Warrendale: TMS, 2011), pp. 569–574.
12. M. Dupuis and R.D. Peterson, *Light Metals*, ed. R.D. Peterson (Warrendale: TMS, 2000), pp. 169–178.
13. J. Dreyfus, L. Rivoaland, and S. Lacroix, *Light Metals*, ed. A.T. Tabereaux (Warrendale: TMS, 2004), pp. 603–608.
14. M. Blais, M. Desilets, and M. Lacroix, *Appl. Therm. Eng.* 58, 439 (2013).
15. S. Das, G. Brooks, and Y. Morsi, *Metall. Trans. B* 42, 243 (2011).
16. J. Zoric, J. Thonstad, and T. Haarberg, *Metall. Trans. B* 30, 341 (1999).
17. H. Fortin, N. Kandev, and M. Fafard, *Finite Elem. Anal. Des.* 52, 71 (2012).
18. N.X. Feng, J.P. Peng, Y.W. Wang, Y.Z. Di, and X.A. Liao, *Light Metals*, ed. B. Sadler (Warrendale: TMS, 2012), pp. 549–552.
19. N. Feng, China Patent, CN 102400176A, 2012/04/04.
20. N. Feng, *Aluminum Electrolysis*, 188 (2006).
21. P. Reny and S. Wilkening, *Light Metals*, ed. D.P. Peterson (Warrendale: TMS, 2000), pp. 1005–1010.
22. H.A. Øye and B.J. Welch, *JOM* 50, 18 (1998).
23. D. Lombard, T. Beheregaray, B. Feve, and J.M. Jolas, *Light Metals*, ed. B.J. Welch (Warrendale: TMS, 1998), pp. 653–658.